NAVAL SHIP RESEARCH AND DEVELOPMENT CENTER
Washington, D.C. 20007



# EVALUATION OF EFFECT OF BOW FORM ON MODEL WAVE-INDUCED AND WHIPPING RESPONSES





STRUCTURAL MECHANICS LABORATORY

**RESEARCH AND DEVELOPMENT REPORT**

February 1968 Report 2556

The Naval Ship Research and Development Center is a U.S. Navy center for laboratory effort directed at achieving improved sea and air vehicles. It was formed in March 1967 by merging the David Taylor Model Basin at Carderock, Maryland and the Marine Engineering Laboratory at Annapolis, Maryland. The Mine Defense Laboratory, Panama City, Florida became part of the Center in November 1967.

Naval Ship Research and Development Center
Washington, D. C. 20007

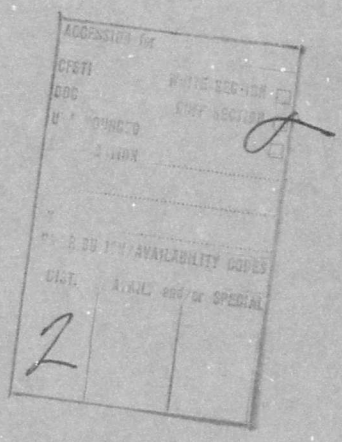

# EVALUATION OF EFFECT OF BOW FORM ON MODEL WAVE-INDUCED AND WHIPPING RESPONSES

by

John N. Andrews and

Alfred L. Dinsenbacher

## ABSTRACT

Random wave tests were conducted with a model of an aircraft carrier and with the forward bow sections of the carrier model modified in the form of a V. The models were tested in random waves representing various sea states at speeds of 0 and 13.8 knots (full-scale). Tests were conducted in head seas only.

Response amplitude operators (RAOs) for wave-induced midship bending moment and pitch angle were derived from spectral analysis. Comparison of the RAOs showed little difference due to change in bow form. The comparison of whipping response for both models showed little difference at zero speed; however, at 13.8 knots, the whipping response for the carrier model increased greatly from the zero speed test while the V-form model showed little difference.

## ADMINISTRATIVE INFORMATION

The work reported here was authorized by NAVSEC letter F013 03 01 Serial 442-109 of 8 July 1963 and was funded under Subproject S-F013 03 01, Task 1973.

BLANK PAGE

TABLE OF CONTENTS



LIST OF FIGURES

## NOTATION

| | |
|---|---|
| $B$ | Ship breadth amidship (103 ft) |
| $g$ | Acceleration due to gravity |
| $L_s$ | Ship length between perpendiculars (820 ft) |
| $\rho$ | Mass density of sea water |
| $\omega_L$ | Frequency of wave equal to ship length |
| $\omega_w$ | Wave frequency |
| $\Omega = \frac{\omega_w}{\omega_L}$ | Nondimensional frequency |

## INTRODUCTION

This report is one of a series on the results of tests of a segmented model designed to correlate full-scale, model, and computer programs.[1,2,4,6] The objective of this report is to evaluate the effect of change in bow form on ship response, i.e., the pitch angle, the wave-induced bending moment, and in particular, the whipping response of the hull girder. To accomplish the program, a 6-foot model of an ESSEX-Class carrier (scale ratio $\lambda$ = 136) was constructed together with two additional bow sections having V- and U-forms. A detailed description of the carrier model and the instrumentation employed to record the measurements is given elsewhere.[3,4] The scaling laws applicable are based upon the well-known Froude principle.[3] The three models were tested in the 140-foot basin for a variety of wave conditions, both regular and random, at speeds of 0 and 13.8 knots (full-scale), Froude number of 0.14. The mass-elastic properties (i.e., the weight distribution and vertical bending rigidity) for the three models were kept the same. Regular wave test results for the carrier model and V-bow modification have been reported elsewhere.[4,5] The U-bow regular wave test results will be published in a future NSRDC report. This report presents results for random wave tests of the carrier and V-bow models; their lines are shown in Figures 1 and 2.

## MODEL TEST PROGRAM AND DATA ANALYSIS

The carrier and V-bow models were tested in the 140-foot basin at the Center. The models were free to heave and pitch but were constrained in yaw, sway, surge, and roll.

Random waves corresponding to State 6, 7, 8, and 9 seas were generated by manually varying the frequency and amplitude controls of the wavemaker. The models were tested in each sea condition at speeds of 0 and 13.8 knots. Only head sea tests were performed. Since the random waves were generated manually, corresponding sea states for each model vary to some degree in location of peak frequency and amplitudes (see Figures 3 to 12).

---

[1]References are listed on page 16.

Data obtained for the carrier and V-bow models were subjected to spectral analysis from which response amplitude operators (RAOs)[4] for midship bending moment and pitch angle were derived. The RAOs are defined as the ratio of the response to the wave spectral densities at corresponding frequencies. The $\sqrt{RAO}$ amplitudes for all wave conditions were then averaged.[7]

Inasmuch as model validity has been demonstrated in a previous report,[6] the results presented here are considered applicable to prototype ships with similar lines. All values reported herein are given in terms of full-scale units as related to the carrier ESSEX.

## RESULTS AND DISCUSSION

### ORDINARY WAVE-INDUCED RESPONSE

Figures 13 to 16 present the average $\sqrt{RAOs}$ for wave-induced bending moment and pitch angle for 0- and 13.8-knot speeds, respectively, for the V-bow and carrier model. These figures indicate that these RAOs are independent of bow form.

In Figures 17 to 20, the root mean square amplitude (RMS)[4] or $\sqrt{E^*}$ of response is shown plotted as a function of RMS wave amplitude. These plots permit comparison of responses for the V-bow and carrier. Since the RAOs are virtually independent of bow form, the differences in $\sqrt{E}$ response values for the V-bow and carrier model can be attributed to the difference in the wave characteristics, i.e., since the random waves were generated manually, it was difficult to obtain identical wave spectra.

### WHIPPING RESPONSES

Figures 21 and 22 are sample oscillograms of slamming events for the V-bow and carrier models, respectively, in waves corresponding to those shown in Figure 8. Figures 23 and 24 show the ratio of maximum whipping response to the $\sqrt{E}$ of wave-induced response for each wave condition and speed.

---

*E is the mean square amplitude and is equal to the area under the spectrum.

It may be noted in these figures that only four points are plotted for the V-bow results. The last point was omitted because during the highest wave test generated, the model struck the stops on the heave post, causing a violent impact which produced an erroneous response in the model. The fact that the second point in the carrier whipping response was larger than expected is attributed to the phasing between ship and wave motion and the past history of the whipping response which reinforced the next whipping event.

There was little difference in the whipping response at zero speed, despite the marked difference in bow form (see Figures 1 and 2). The carrier bow has a large flare which begins above the design waterline. Whipping response is considered to be primarily due to bow flare slamming and not bottom slamming. It is realized of course that bottom slamming does contribute to whipping but, since both models have the same form below the design waterline except at the extreme forward end, the difference in whipping response is attributed to the differences in bow form above the design waterline. The relative vertical velocity of the bow with respect to the waves was small for the zero speed tests, hence the impact force on the carrier flared portion was mild. However, it was quite evident at 13.8 knots that the carrier exhibited larger whipping response than the V-bow model (Figure 24). Actually speed appeared to have little effect on the whipping response of the V-bow model. However, the increase in the whipping response with speed observed from the carrier results can be attributed in part to the larger relative velocity of the bow with respect to the wave which caused a much more severe impact force on the flared portion of the bow.

An estimate of the structural damping, as determined from the log decrement, was $0.05 \pm 0.01$ for both models. This value agrees with that of 0.04 obtained from the prototype ship.

The total double amplitude maximum moment (whipping plus wave induced) is plotted in Figures 25 and 26, as a function of $\sqrt{E}$ wave amplitude for 0 and 13.8 knots, respectively. Plots in this form are useful since they give the ship designer an estimate of the total moment a ship may encounter in a given sea state. The predicted maximum peak-to-peak wave-induced moment is compared with the measured maximum wave-induced

moments in Table 1. The predicted[4] maximum wave-induced moment is obtained from the following:

$$M_{max} = 2\sqrt{E \log_e N}$$

where E is the area under the spectrum and N is the number of variations in a record. The predicted values shown in Table 1 were derived by assuming N is 200 or about half an hour in time. The horizontal line in the figures is the hog to sag moment for which the carrier was designed based upon a L/20 wave. This is shown to permit estimating the adequacy of ship design. At zero ship speed, the intersection of the design moment line with the total moment (for V-bow and carrier) occurs in a high State 7 sea (Figure 25) whereas at 13.8 knots, the point of intersection for the carrier data occurs in a low State 7 sea (Figure 26). Thus an increase in ship speed causes the point of intersection to occur in a lower sea state. This type of presentation can provide a useful basis for design criteria. Of course, many more tests of prototypes and models need to be made before this method can be considered completely acceptable since only head sea tests were conducted.

## CONCLUSIONS

1. Bow form had little effect on the RAOs for bending moment. Although Figures 13 to 16 indicated that the effect of speed on the RAOs was insignificant up to 13.8 knots, more information is required to determine the effect at higher ship speeds. However, the 140-foot basin is not well suited for random wave tests at higher speeds.

2. Wave-induced bending moment and pitch angle response were not affected by ship speed or bow form (Figures 17 to 20). Any differences can be attributed to the differences in the generated waves.

3. There was little or no difference in whipping response for the two models at zero speed. At 13.8 knots, however, the whipping response of the carrier model was greatly affected whereas that of the V-bow showed little difference when compared with the zero speed results (Figures 23 and 24).

## ACKNOWLEDGMENTS

The authors wish to thank Mr. J. Oglesby, Mr. D. Pincus, and Mr. D. Hill for their assistance in developing a program in conjunction with the Applied Mathematics Laboratory for computing response amplitude operators directly. This effort saved considerable hand calculations and resulted in a large saving in time.

The assistance of Mr. A.V. Davis and Mr. E.A. Zwenig during the testing phase of the program was very helpful.

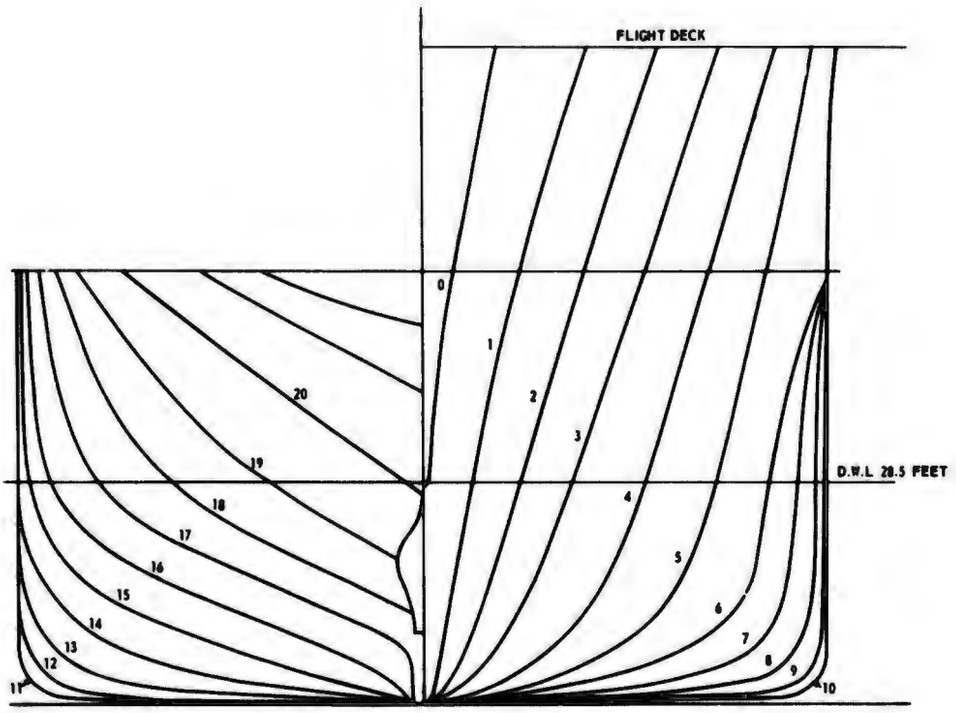


Figure 1 - Lines of V-Bow

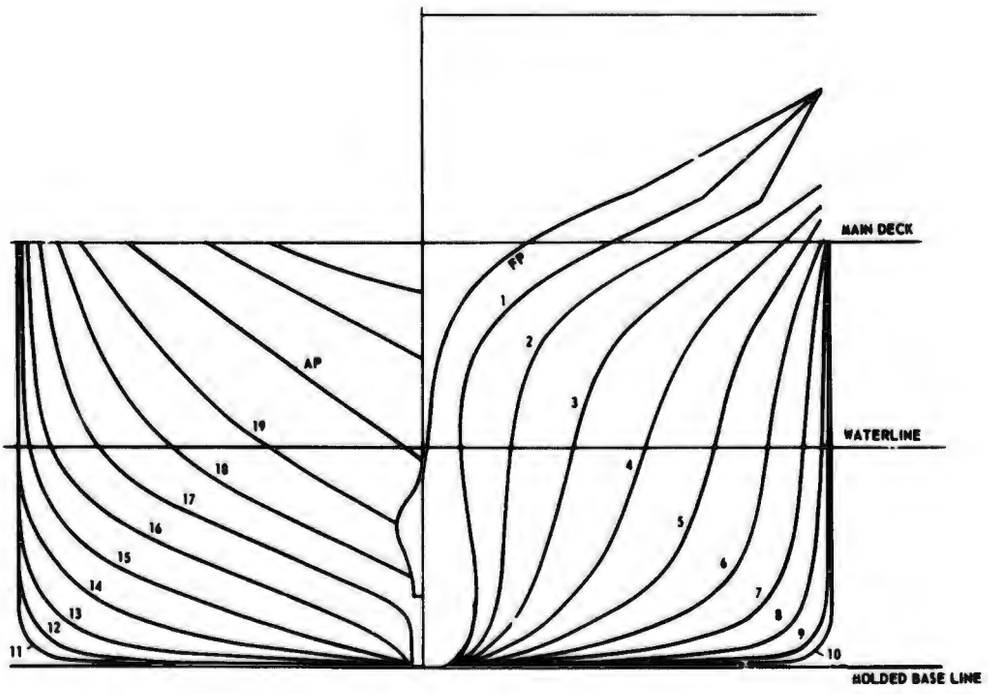


Figure 2 - Lines of ESSEX

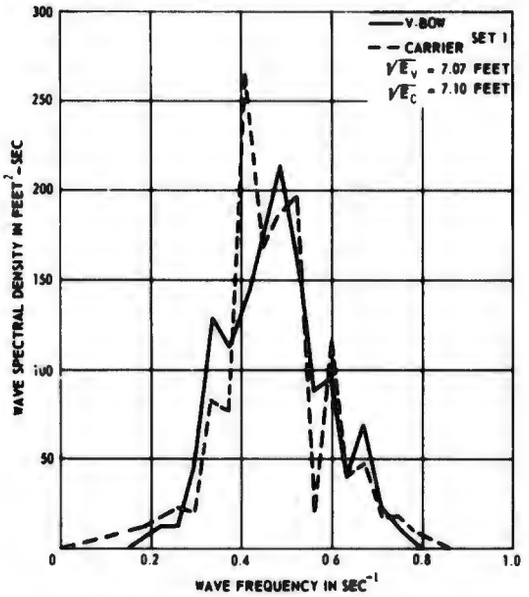


Figure 3 - Wave Spectra for Zero Speed, State 6 Sea

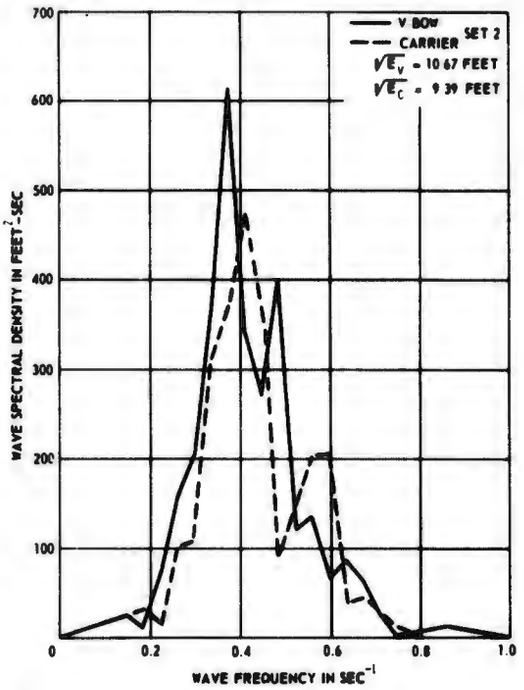


Figure 4 - Wave Spectra for Zero Speed, State 7 Sea

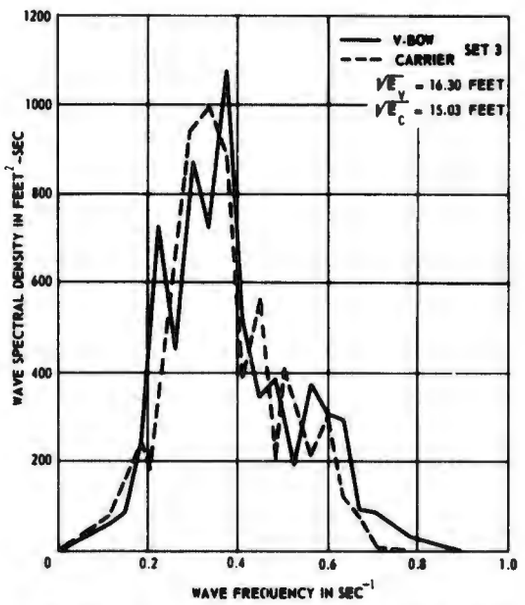


Figure 5 - Wave Spectra for Zero Speed, Low State 8 Sea

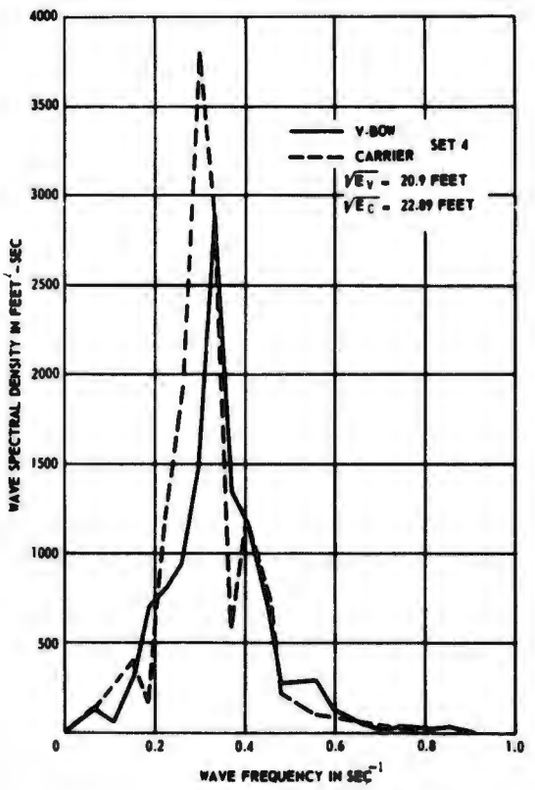


Figure 6 - Wave Spectra for Zero Speed, High State 8 Sea

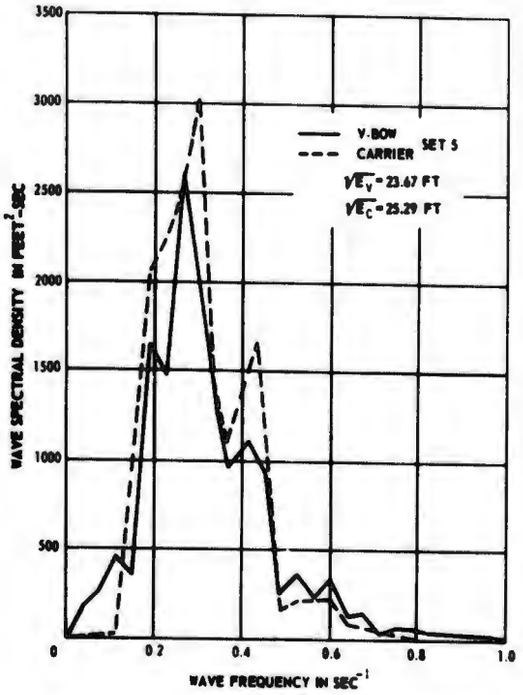


Figure 7 - Wave Spectra for Zero Speed, State 9 Sea

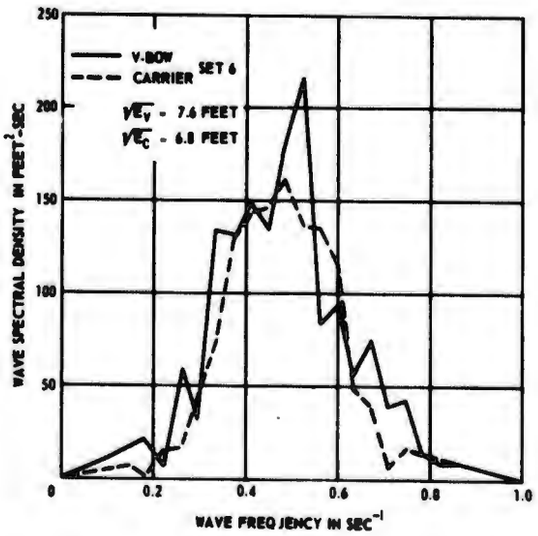


Figure 8 - Wave Spectra for 13.8-Knot Speed, State 6 Sea

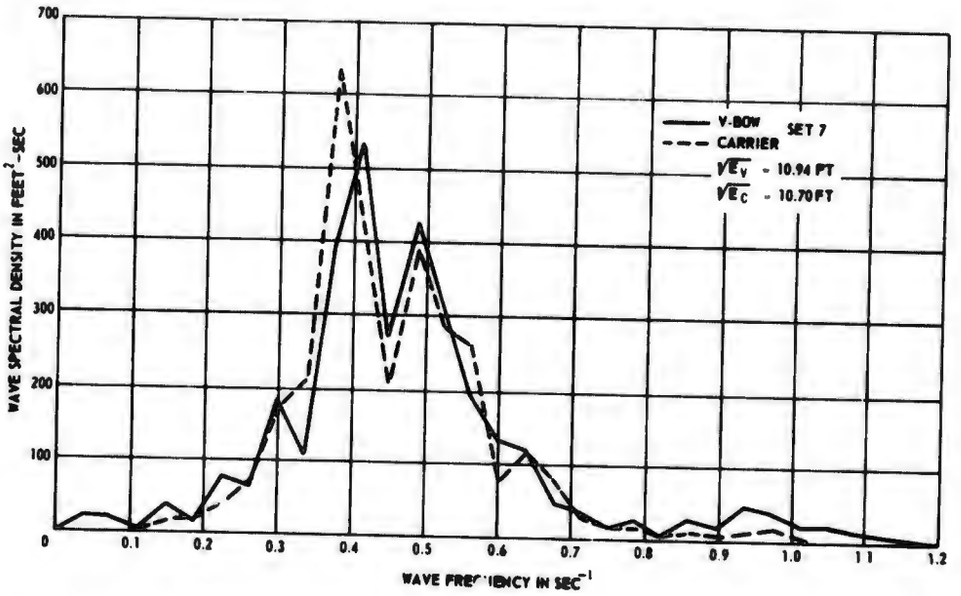


Figure 9 - Wave Spectra for 13.8-Knot Speed, State 7 Sea

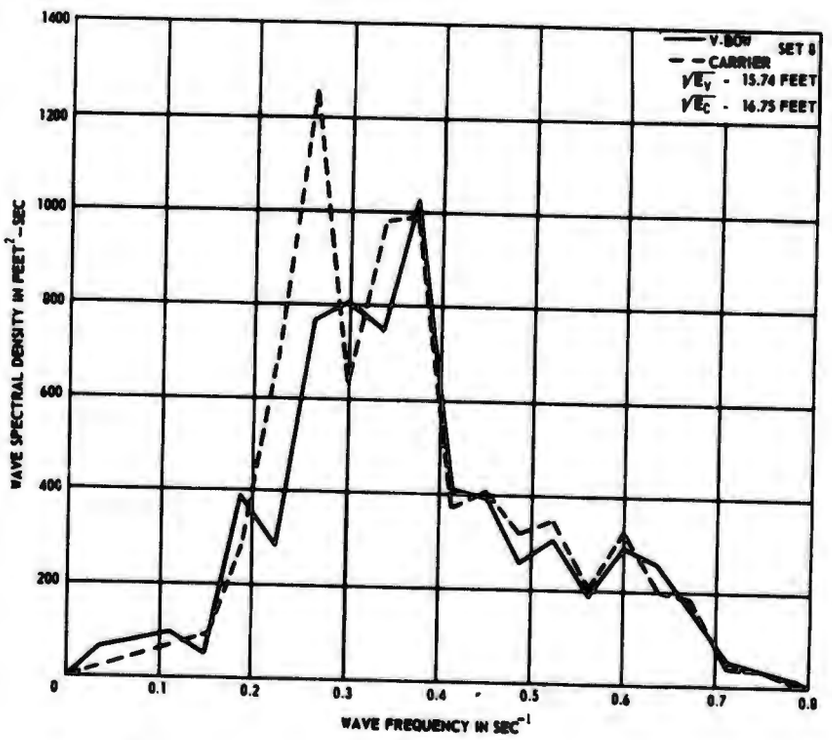


Figure 10 - Wave Spectra for 13.8-Knot Speed, Low State 8 Sea

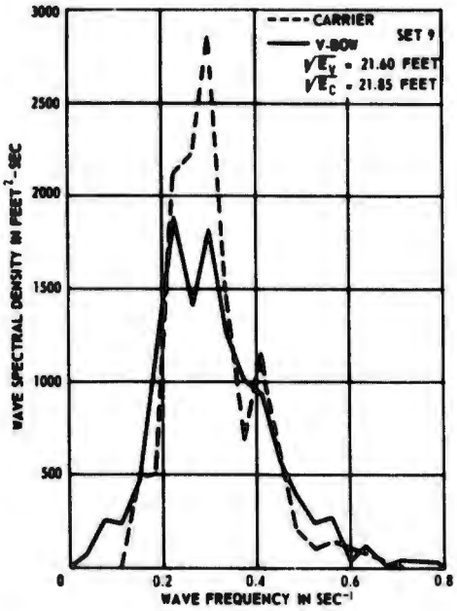


igure 11 - Wave Spectra for 13.8-Knot Speed, High State 8 Sea

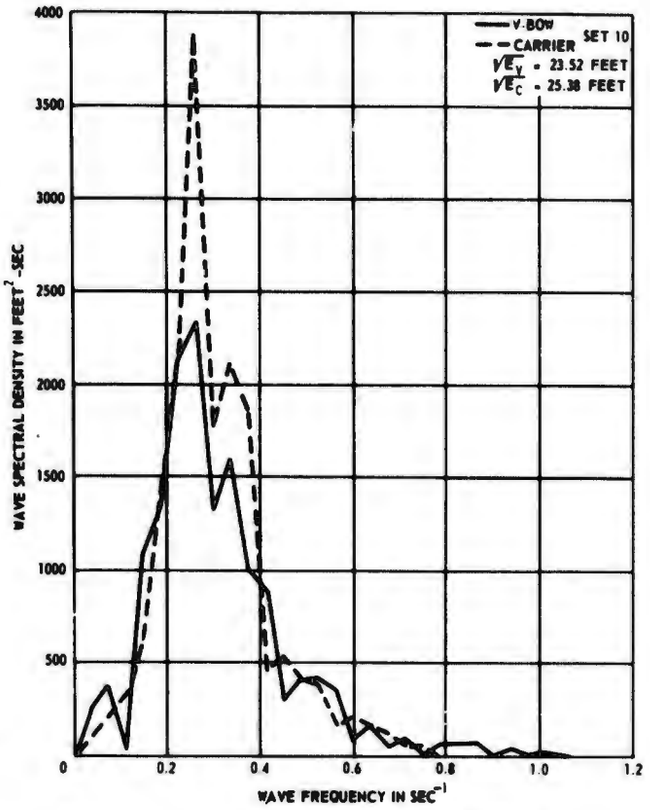


Figure 12 - Wave Spectra for 13.8-Knot Speed, State 9 Sea

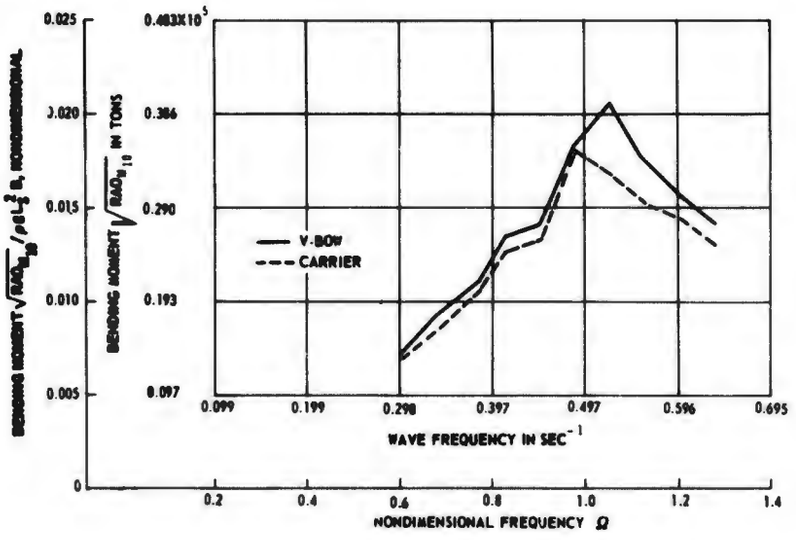


Figure 13 - Square Root of Bending Moment $RAO_{M_{10}}$ for Zero Speed

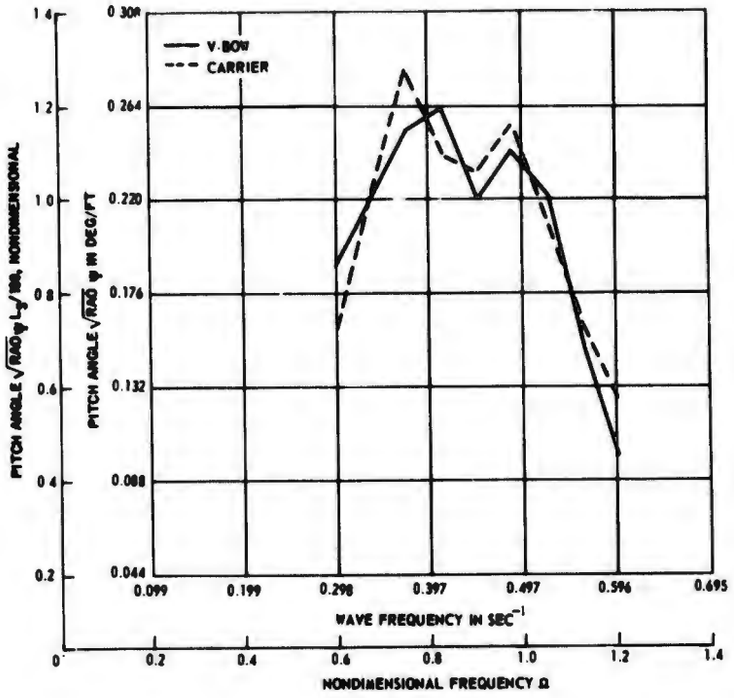


Figure 14 - Square Root of Pitch Angle $RAO_\psi$ for Zero Speed

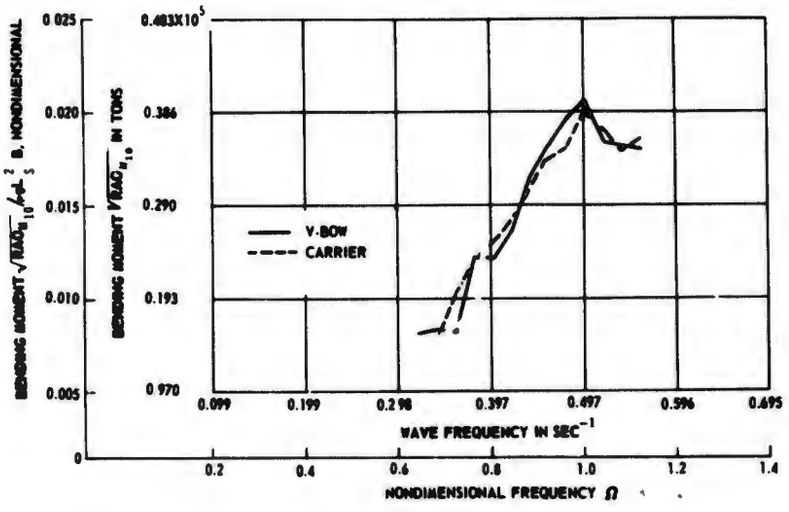


Figure 15 - Square Root of Bending Moment $RAO_{M_{10}}$ for 13.8-Knot Speed

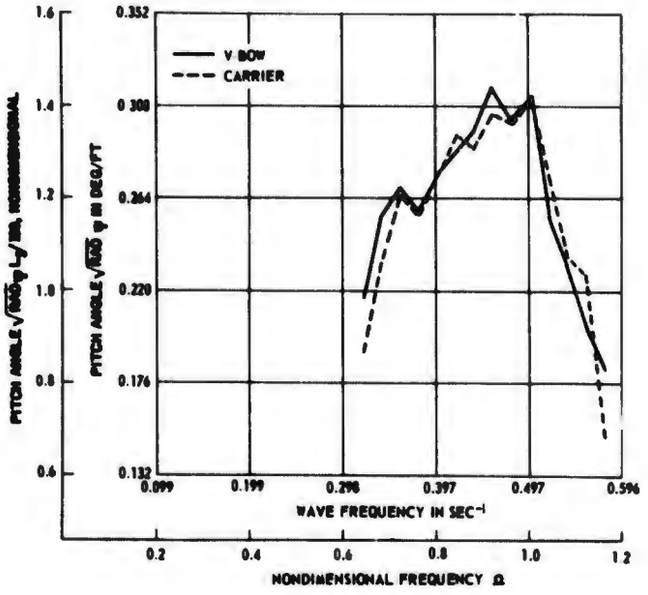


Figure 16 - Square Root of Pitch Angle $RAO_{\psi}$ for 13.8-Knot Speed

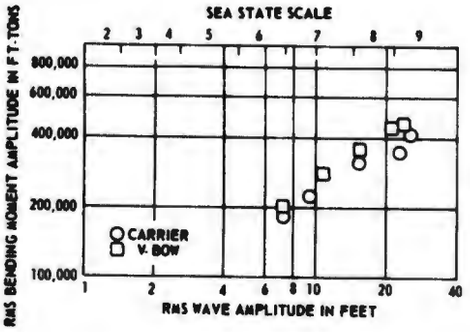


Figure 17 - RMS Bending Moment Amplitude as a Function of RMS Wave Amplitude for Zero Speed

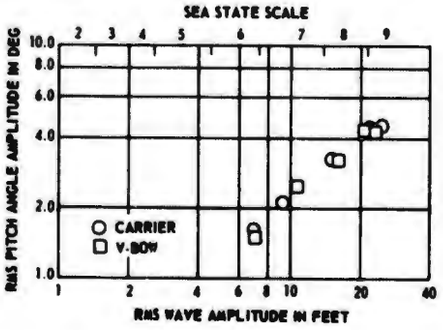


Figure 18 - RMS Pitch Angle Amplitude as a Function of RMS Wave Amplitude for Zero Speed

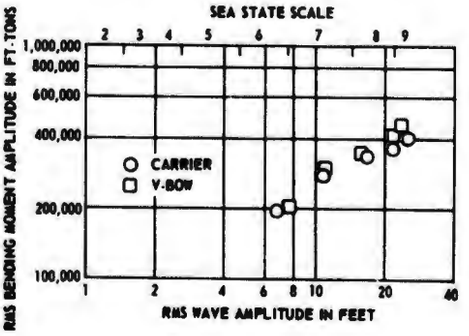


Figure 19 - RMS Bending Moment Amplitude as a Function of RMS Wave Amplitude for 13.8-Knot Speed

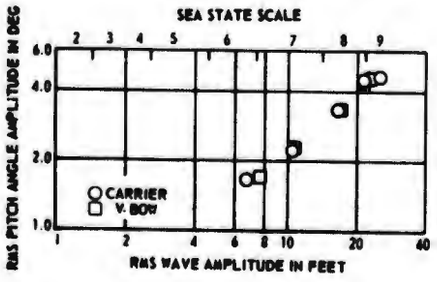


Figure 20 - RMS Pitch Angle Amplitude as a Function of RMS Wave Amplitude for 13.8-Knot Speed

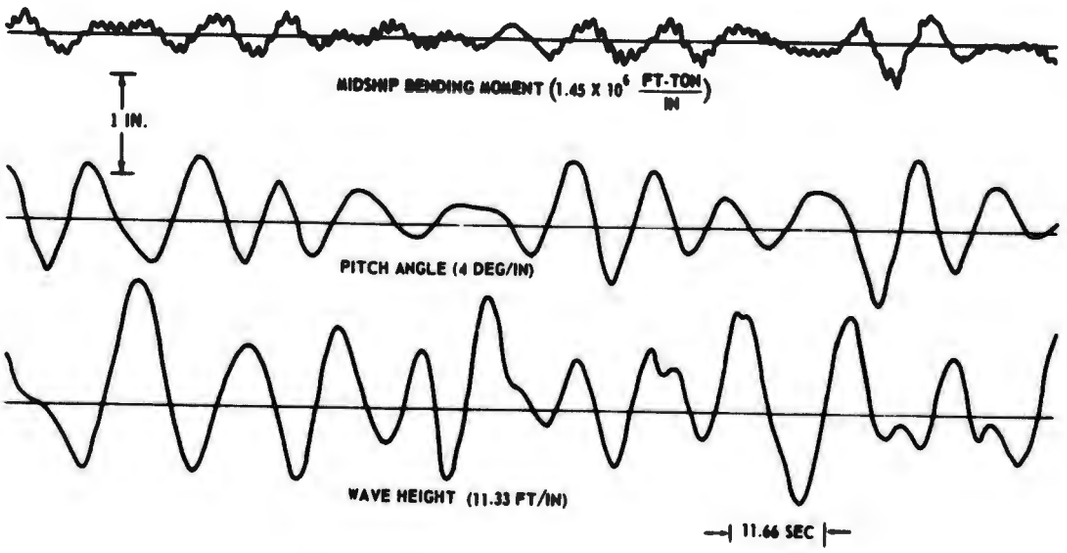


Figure 21 - Sample Oscillogram from V-Bow Model Test

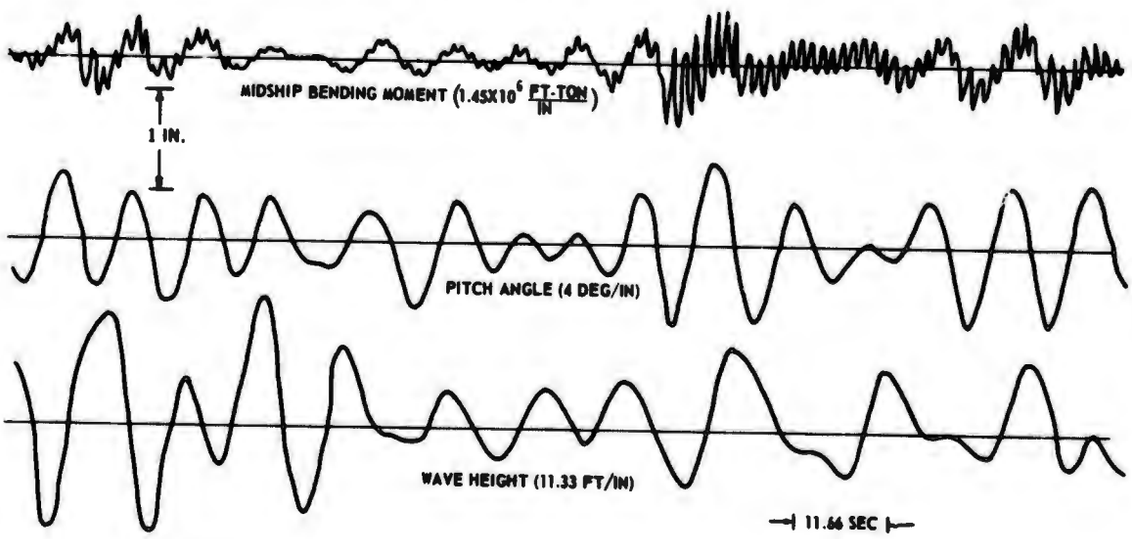


Figure 22 - Sample Oscillogram from Carrier Model Test

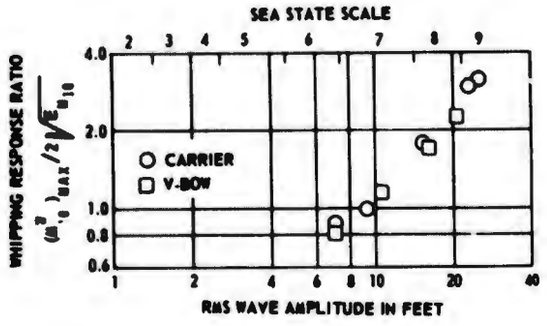


Figure 23 - Whipping Response Ratio as a Function of RMS Wave Amplitude for Zero Speed

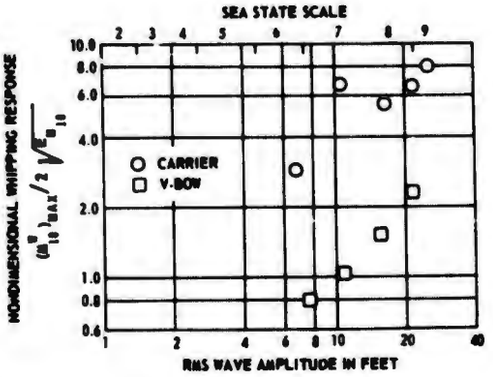


Figure 24 - Whipping Response Ratio as a Function of RMS Wave Amplitude for 13.8-Knot Speed

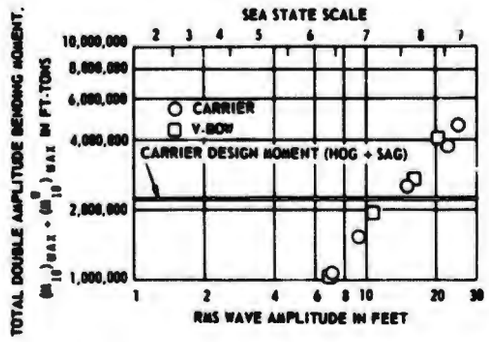


Figure 25 - Total Double Amplitude Bending Moment as a Function of RMS Wave Amplitude for Zero Speed

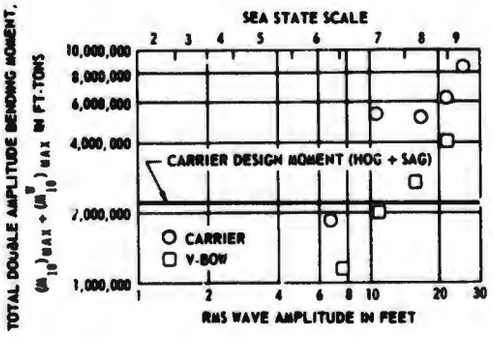


Figure 26 - Total Double Amplitude Bending Moment as a Function of RMS Wave Amplitude for 13.8-Knot Speed

## TABLE 1

### Wave and Response Information

| | Set | RMS Wave Amplitude $\sqrt{E_{H_w}}$ ft | | RMS Moment Amplitude $\sqrt{E_{M_{10}}} \times 10^{-5}$ ft-tons | | RMS Pitch Angle Amplitude $\sqrt{E_{\psi}}$ deg | | Whipping Moment Double Amplitude $M_{10}^{W} \times 10^{-5}$ ft-tons | | Total Measured Maximum Moment Double Amplitude $M_{10}^{T} \times 10^{-5}$ ft-tons | | Measured Maximum Wave-Induced Moment Double Amplitude $M_{max}^{M} \times 10^{-5}$ ft-tons | | Predicted Maximum Wave-Induced Moment Double Amplitude $M_{max}^{P} \times 10^{-5}$ ft-tons | |
|---|---|---|---|---|---|---|---|---|---|---|---|---|---|---|---|
| | | V-Bow | Carrier | V-Bow | Carrier | V-Bow | Carrier | V-Bow | Carrier | V-Bow | Carrier | V-Bow | Carrier | V-Bow | Carrier |
| $V_s$ = 0 | 1 | 7.07 | 7.10 | 1.98 | 1.81 | 1.44 | 1.64 | 3.18 | 3.18 | 11.43 | 10.58 | 8.25 | 7.40 | 9.10 | 8.32 |
| | 2 | 10.67 | 9.39 | 2.78 | 2.48 | 2.46 | 2.20 | 6.37 | 4.93 | 19.25 | 15.53 | 12.88 | 10.60 | 12.78 | 11.40 |
| | 3 | 16.3 | 15.03 | 3.55 | 3.13 | 3.21 | 3.25 | 12.16 | 11.00 | 27.22 | 25.20 | 15.06 | 14.20 | 16.34 | 14.40 |
| | 4 | 20.9 | 22.89 | 4.41 | 3.48 | 4.26 | 4.41 | 19.98 | 20.30 | 40.39 | 37.80 | 20.41 | 17.50 | 20.28 | 14.64 |
| | 5 | 23.67 | 25.29 | 4.58 | 4.13 | 4.26 | 4.49 | --- | 25.8 | --- | 46.00 | 23.74 | 20.20 | 21.06 | 19.00 |
| $V_s$ = 13.6 knots | 6 | 7.6 | 6.8 | 2.11 | 1.96 | 1.70 | 1.68 | 3.33 | 11.30 | 11.73 | 18.54 | 8.40 | 7.24 | 9.70 | 9.02 |
| | 7 | 10.94 | 10.70 | 2.93 | 2.77 | 2.59 | 2.51 | 6.08 | 36.40 | 19.98 | 50.30 | 13.90 | 13.90 | 13.48 | 12.76 |
| | 8 | 15.74 | 16.75 | 3.53 | 3.38 | 3.35 | 3.38 | 10.64 | 37.30 | 27.44 | 51.60 | 16.50 | 14.30 | 16.24 | 15.54 |
| | 9 | 21.60 | 21.85 | 4.15 | 3.64 | 4.43 | 4.46 | 19.11 | 47.80 | 40.17 | 63.40 | 21.06 | 15.60 | 19.10 | 16.74 |
| | 10 | 23.52 | 25.38 | 4.60 | 4.04 | 4.77 | 4.69 | --- | 64.30 | --- | 84.70 | 20.85 | 20.40 | 21.16 | 19.58 |

## REFERENCES

1. Andrews, J.N., "A Method for Computing the Response of a Ship to a Transient Force," David Taylor Model Basin Report 1544 (Nov 1963).

2. Andrews, J.N. and Chuang, S.L., "Seaworthiness Analog Computer," David Taylor Model Basin Report 1829 (Aug 1965).

3. Andrews, J.N. and Church, J.W., "A Model for the Simulation of Wave Impact Loads and Resulting Transient Vibration of a Naval Vessel," Trans. ASME, pp. 16-27 (1963).

4. Andrews, J.N. and Dinsenbacher, A.L., "Structural Response of a Carrier Model in Regular and Random Waves," David Taylor Model Basin Report 2177 (Apr 1966).

5. Davis, A.V., "Hull Girder Response of a Carrier Model with a Modified V-Bow in Regular and Random Head Waves," NSRDC Report 2508 (Oct 1967).

6. Andrews, J.N. and Dinsenbacher, A.L., "Agreement of Model and Prototype Response Amplitude Operators and Whipping Response," NSRDC Report 2351 (May 1967).

7. Andrews, J.N. and Dinsenbacher, A.L., "Response Amplitude Operators and Whipping Response of a Carrier Model in Random Waves," NSRDC Report 2522 (Jan 1968).

UNCLASSIFIED

Security Classification

**DOCUMENT CONTROL DATA - R & D**

*Security classification of title, body of abstract and indexing annotation must be entered when the overall report is classified)*

1 ORIGINATING ACTIVITY *(Corporate author)*

Naval Ship R&D Center
Washington, D.C. 20007

2a. REPORT SECURITY CLASSIFICATION

Unclassified

2b. GROUP

3 REPORT TITLE

EVALUATION OF EFFECT OF BOW FORM ON MODEL WAVE-INDUCED AND WHIPPING RESPONSES

4 DESCRIPTIVE NOTES *(Type of report and inclusive dates)*

Final

5 AUTHOR(S) *(First name, middle initial, last name)*

John N. Andrews and Alfred L. Dinsenbacher

| 6 REPORT DATE | 7a. TOTAL NO. OF PAGES | 7b. NO. OF REFS |
|---|---|---|
| February 1968 | 21 | 7 |

| 8a. CONTRACT OR GRANT NO | 9a. ORIGINATOR'S REPORT NUMBER(S) |
|---|---|
| b. PROJECT NO. S-F013 03 01 | 2556 |
| c. Task 1973 | 9b. OTHER REPORT NO(S) *(Any other numbers that may be assigned this report)* |
| d. | |

10 DISTRIBUTION STATEMENT

This document is subject to special export controls and each transmittal to foreign governments or foreign nationals may be made only with prior approval of CO & DIR, Naval Ship Research and Development Center.

| 11. SUPPLEMENTARY NOTES | 12. SPONSORING MILITARY ACTIVITY |
|---|---|
| | Naval Ship Engineering Center |

13 ABSTRACT

Random wave tests were conducted with a model of an aircraft carrier and with the forward bow sections of the carrier model modified in the form of a V. The models were tested in random waves representing various sea states at speeds of 0 and 13.8 knots (full-scale). Tests were conducted in head seas only.

Response amplitude operators (RAOs) for wave-induced midship bending moment and pitch angle were derived from spectral analysis. Comparison of the RAOs showed little difference due to change in bow form. The comparison of whipping response for both models showed little difference at zero speed; however, at 13.8 knots, the whipping response for the carrier model increased greatly from the zero speed test while the V-form model showed little difference.

DD FORM 1 NOV 68 1473 (PAGE 1)

S/N 0101-807-6801



UNCLASSIFIED

Security Classification

| 14 KEY WORDS | LINK A | | LINK B | | LINK C | |
|---|---|---|---|---|---|---|
| | ROLE | WT | ROLE | WT | ROLE | WT |
| Seaworthiness | | | | | | |
| RAO | | | | | | |
| Carrier Model | | | | | | |
| Carrier Model with V-Bow Modification | | | | | | |
| Ordinary Wave-Induced Response | | | | | | |
| Whipping Response | | | | | | |